Supplemental Figure 1

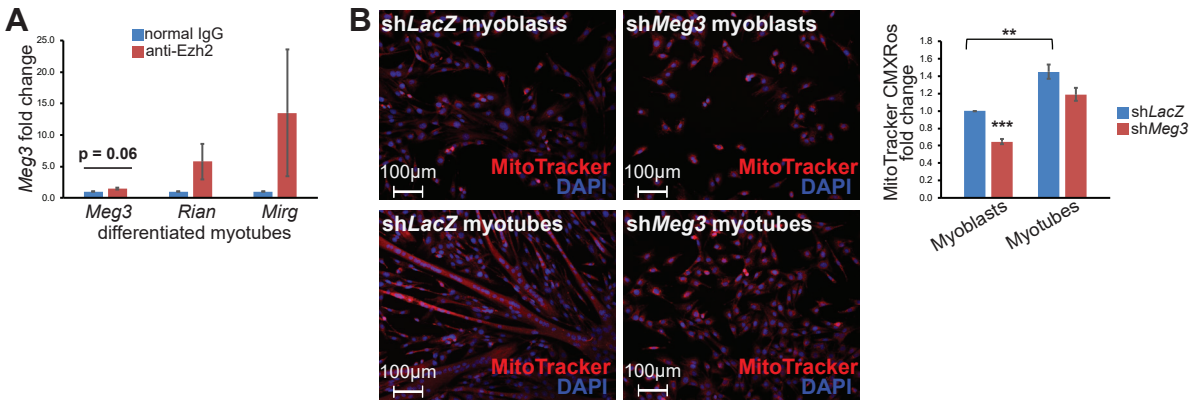

Figure S1: *Meg3* is not significantly immunoprecipitated with Ezh2 in day3 myotubes, and sh*Meg3* myoblasts display reduced mitochondrial mass. A) RNA-IP conducted in differentiated C2C12 myotubes revealed that Ezh2-dependent *Meg3* enrichment is downregulated upon myogenic differentiation (n=3 sets of 10 pooled plates). **B)** C2C12 myoblasts and myotubes were pulsed with MitoTracker CMXRos for 40 minutes, and co-stained with α-actinin. Quantification of Mitotracker (restricted to α-actinin+ cells) indicated reduced mitochondrial signal in sh*Meg3* myoblasts, but not myotubes (n=3). Both treatment groups displayed increased MitoTracker signal with differentiation.

Supplemental Figure 2

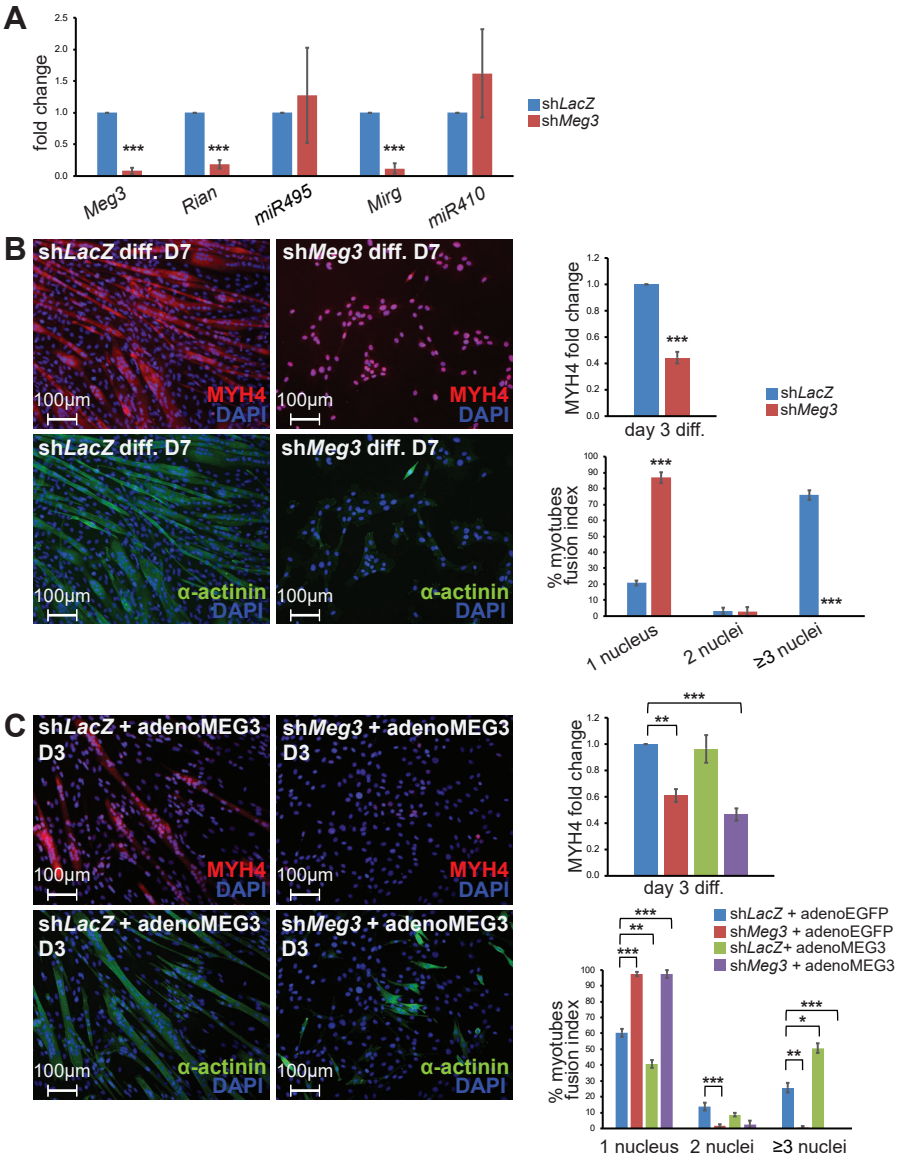

Figure S2: sh*Meg3* knockdown phenotype persists with extended differentiation and transient MEG3 overexpression. A) Expression profiling of *Dlk1-Dio3* ncRNAs revealed significant downregulation of lncRNAs, but not miRNAs (n=3). **B)** Immunofluorescent analysis of shRNA clones on day 7 differentiation revealed persistence of MYH4 and fusion defects in sh*Meg3* C2C12 myotubes. **C)** Transient overexpression of human MEG3 via adenoviral transduction (MOI 60) revealed that the sh*Meg3* phenotype was indifferent to transient overexpression (n=3).

Supplemental Figure 3

Gene name symbol	Gene Name	C2C12		TA	
		Fold Change	p-value	Fold Change	p-value
Mymk	myomaker, myoblast fusion factor	-1.7	0.20	1.2	0.30
Mymx	myomixer, myoblast fusion factor	-1.8	0.22	1.2	0.41
Dysf	dysferlin	-1.9	0.13	-1.3	0.06
Myof	**myoferlin**	-1.4	0.08	**7.5**	**0.00**
Kirrel	**kirre like nephrin family adhesion molecule 1**	**3.5**	**0.00**	**2.3**	**0.00**
Kirrel3	kirre like nephrin family adhesion molecule 3	-1.1	0.73	-1.5	0.29
Kirrel3os	kirre like nephrin family adhesion molecule 3, opposite strand	-1.1	0.91	-1.1	0.82
Jaml	junction adhesion molecule like	-1.2	0.76	1.5	0.12
Jam2	**junction adhesion molecule 2**	**-3.5**	**0.00**	**-1.5**	**0.01**
Jam3	junction adhesion molecule 3	-1.5	0.09	-1.2	0.26
Fer1l5	**fer-1-like 5 (C. elegans)**	**4.8**	**0.01**	1.3	0.56
Ehd1	EH-domain containing 1	1.3	0.39	-1.1	0.37
Ehd2	**EH-domain containing 2**	**2.0**	**0.01**	-1.3	0.14
Ehd4	EH-domain containing 4	-1.3	0.39	1.2	0.20

Figure S3: Myogenic fusion transcripts are not downregulated in sh*Meg3* myotubes. RNAseq data indicated that transcripts of master regulators of myogenic fusion, notably *Myomaker* and *Myomixer*, were not significantly downregulated in sh*Meg3* myotubes.

Supplemental Figure 4

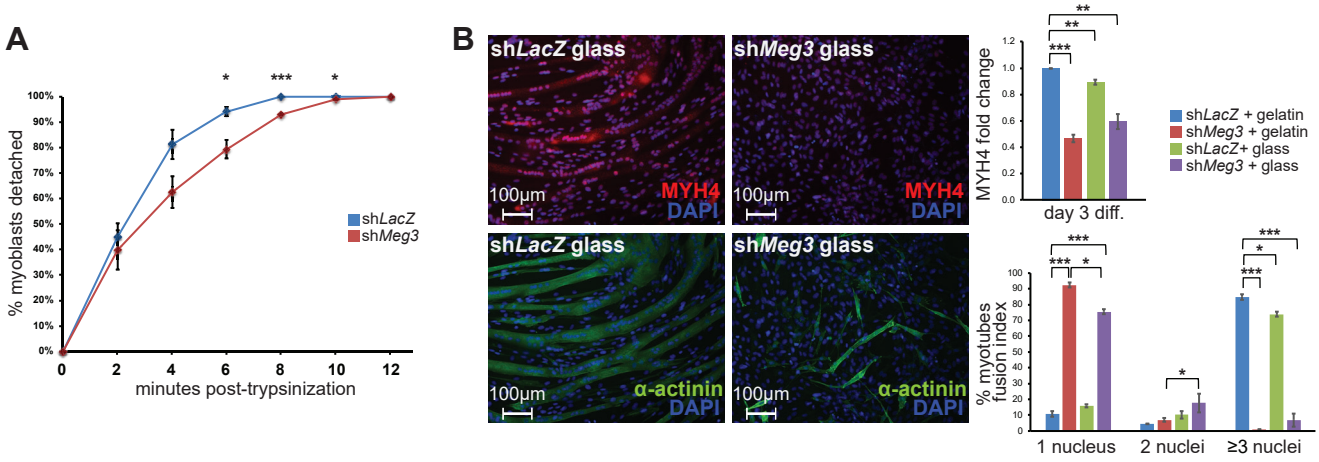

Figure S4: sh*Meg3* myoblasts require longer trypsinzation, and depriving cells of surface substrate had modest effects on fusion. A) Quantification of cells recovered over time during trypsinization revelaed that sh*Meg3* myoblasts require significantly more time to trypsinize to completion (n=3). **B)** When differentiated upon a substrate-deprived surface (glass), sh*Meg3* myoblasts had no change on MYH4 expression (n=3) or fusion of cells with ≥3 nuclei, but did exhibit reduced quantities of myotubes with 1- and 2- nuclei relative to sh*Meg3* controls differentiated on 0.1% gelatin (n=3). Differentiation atop glass also significantly reduced sh*LacZ* MYH4 signal (n=3) and quantity of myotubes with ≥3 nuclei.

Supplemental Figure 5

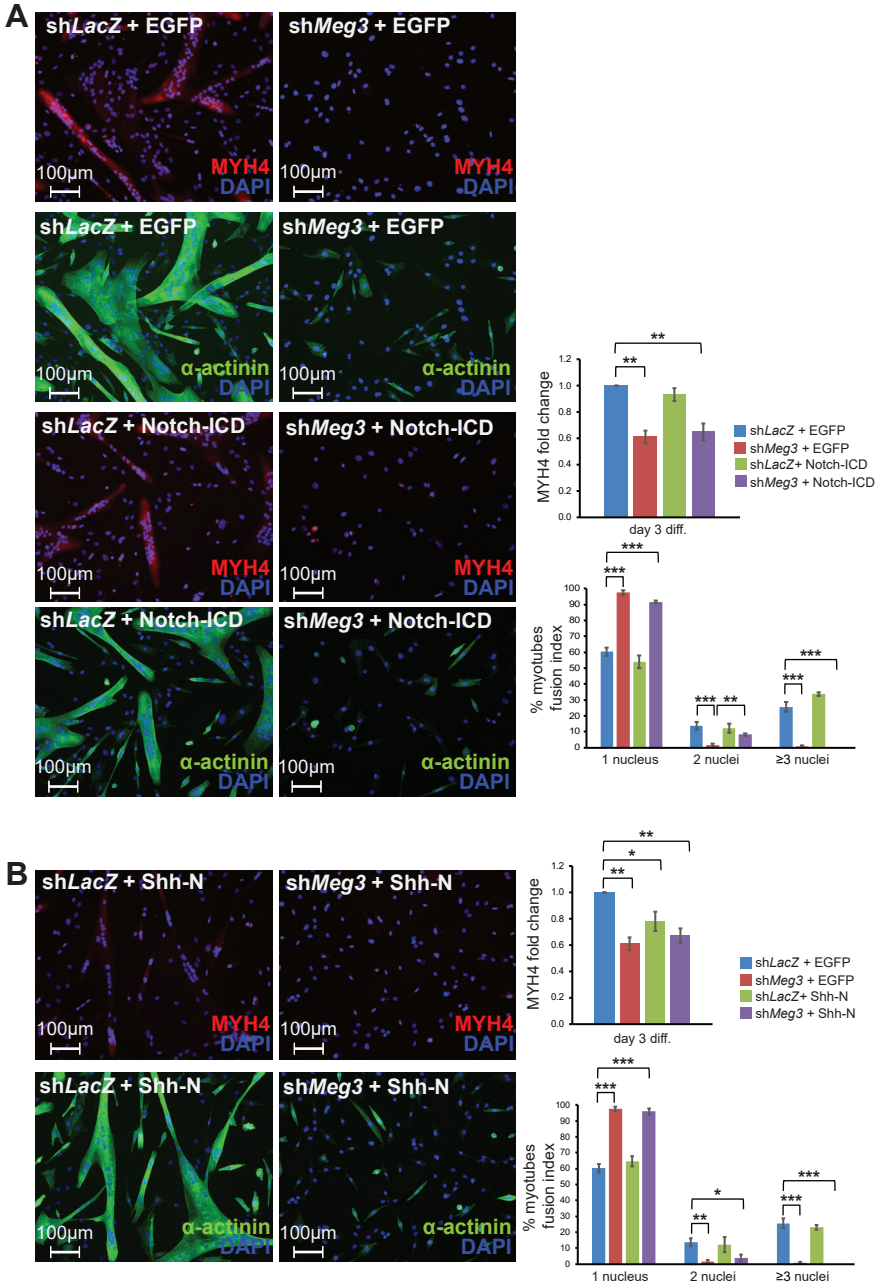

Figure S5: Activation of downregulated pathways Notch and Shh are not sufficient to rescue sh*Meg3* differentiation defects. A) Following adenoviral transduction with adenoEGFP control or adenoNotch-ICD (MOI 25), immunoflurescent analyses revealed no change in MYH4 or fusion (n=3). **B)** Following adenoviral transduction with adenoEGFP control or adenoShh-N (MOI 25), immunoflurescent analyses indicated no change in MYH4 or fusion (n=3).

Supplemental Figure 6

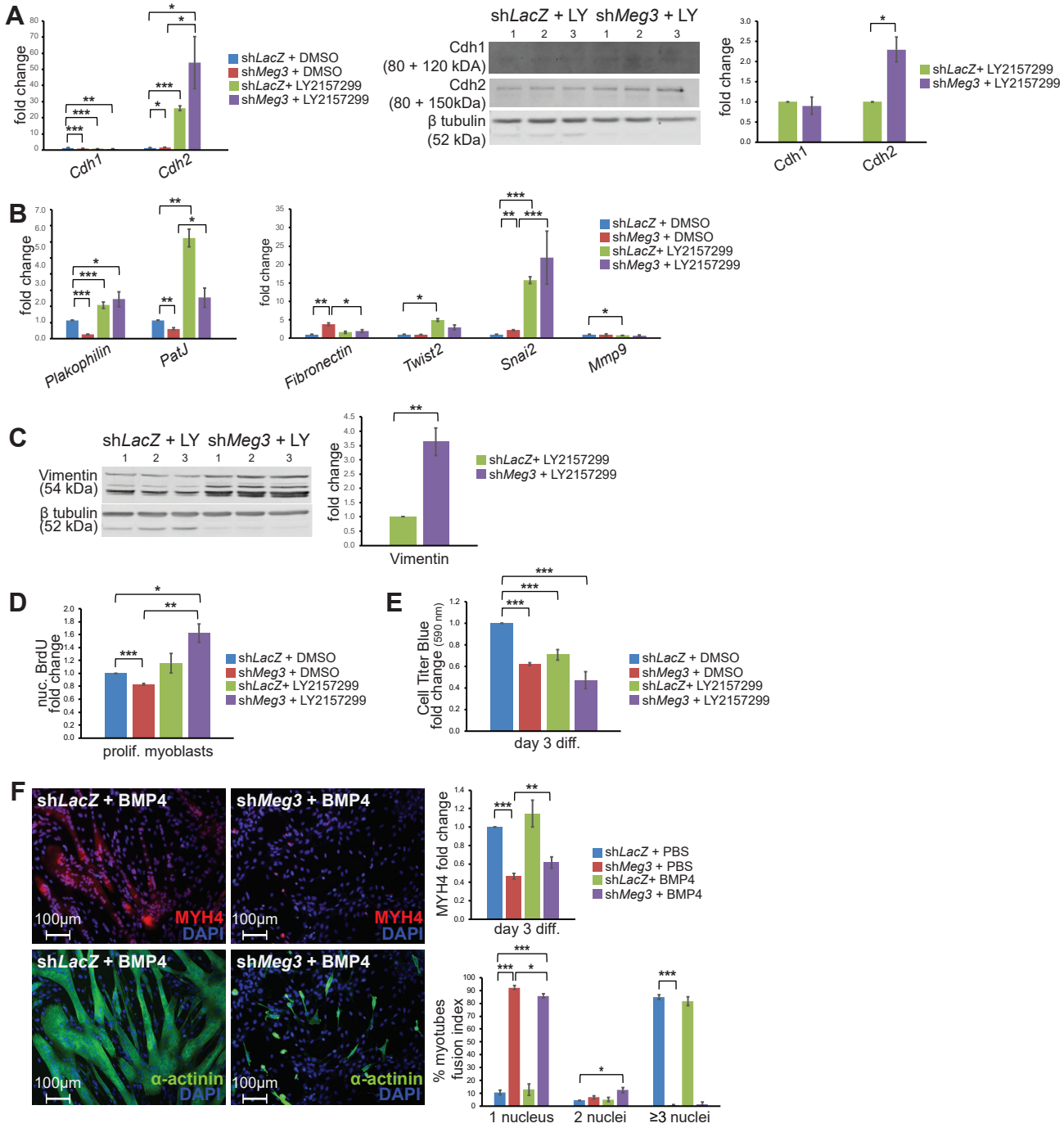

Figure S6: TGFβR1 inhibition results in dynamic EMT marker expression, and BMP4 stimulation is not sufficient for sh*Meg3* rescue. A) qPCR indicated that LY2157299 (LY) treatment resulted in reduced *E-cadherin* (*Cdh1*) transcripts regardless of sh*RNA* treatment, with simultaneous upregulation of *N-cadherin* (*Cdh2*) transcripts (n=3). Western blot revealed modest Cdh1 band detection, and quantification of β-tubulin-normalized signal revealed that LY-treatment enhanced Cdh2 signal in sh*Meg3* myotubes (n=3). **B)** qPCR profiling indicated upregulation of epithelial transcripts *Plakophilin* and *PatJ* regardless of sh*RNA* background (n=3). *Fibronectin* transcript levels returned to normal levels in LY-treated sh*Meg3* myotubes. LY treatment intensified upregulation of *Snai2* transcripts in sh*Meg3* cells, but did not affect *Twist2* or *Mmp9* levels relative to sh*Meg3* myotubes. sh*LacZ* + LY myotubes displayed reduced *Mmp9*, with simultaneous upregulation of *Twist2* when compared to untreated sh*LacZ* cells (n=3). **C)** Western blot quantification of Vimentin suggests that LY treatment enhanced Vimentin expression in sh*Meg3* myotubes relative to LY-treated shLacZ controls (n=3). **D)** Myoblasts pre-treated with 5ng/mL BMP4 (BMP) were subjected to differentiation, and examined for changes in MYH4 expression and fusion index. BMP4 treated sh*Meg3* myotubes had improved MYH4 expression (n=3), reduced mononucleated myotubes, and improved 2-cell fusion, but not ≥3 nuclei fusion.

Supplemental Figure 7

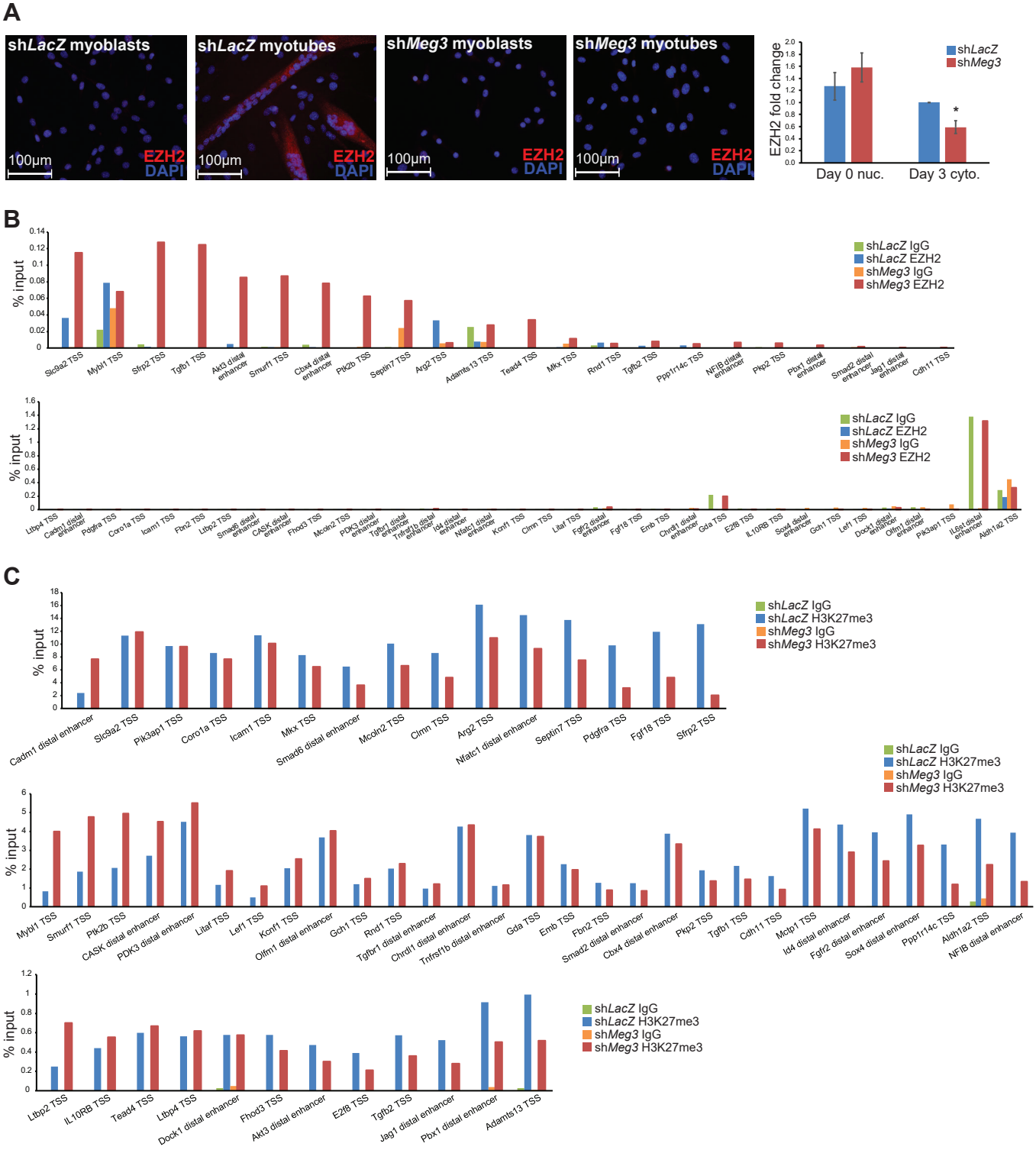

Figure S7: Ezh2 activity is dysregulated in sh*Meg3* C2C12 myoblasts. A) Immunofluorescent analyses of Ezh2 in proliferating myoblasts and day 3 differentiation myotubes indicated cytoplasmic export of Ezh2 with myogenic differentiation; note that these cells were co-stained for H3K27me3, and correspond with images shown in Fig. 9B (n=3). **B)** ChIP-qPCR of Ezh2 immunoprecipitates revealed that Ezh2 immunoprecipitation was only above mock for a subset of loci surveyed, and predominantly enriched in sh*Meg3* samples (n=1 set of 30 pooled plates) **C)** ChIP-qPCR of H3K27me3 immunoprecipitates revealed dynamic changes in H3K27me3 enrichment for 57 loci (n=1 set of 30 pooled plates).

Supplemental Figure 8

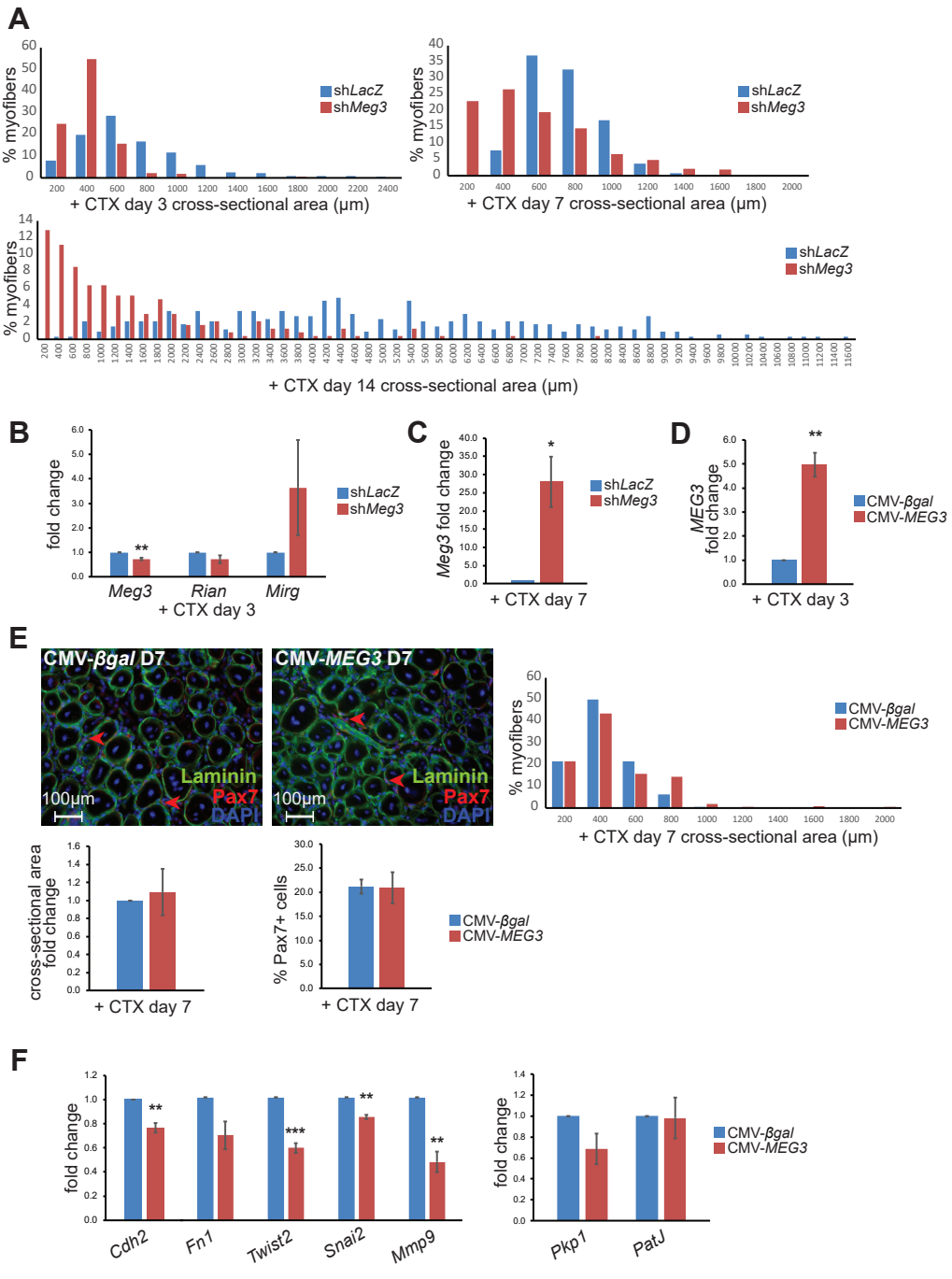

Figure S8: Size and distribution of myofibers, expression profiling, and MEG3 overexpression in TA + CTX muscle. A) Size and distribution of myofibers corroborated cross-sectional area findings shown in Figure 10, with sh*Meg3* muscle harboring increased proportions of small myofibers. **B)** qPCR analysis of *Dlk1-Dio3* lncRNAs suggests adenoviral sh*Meg3* specifically targeted *Meg3*, without affecting other lncRNAs derived from the polycistron at day 3 post-injury (n=3). **C)** At day 7 post-injury, endogenous *Meg3* levels are elevated in sh*Meg3* relative to sh*LacZ* controls (n=3). **D)** Ectopic MEG3 expression was observed in CTX-injured muscle co-treated with CMV-MEG3 adenovirus (n=3). **E)** MEG3 overexpression did not change day 7 + CTX size & distribution of myofibers (right panel), cross-sectional area (bottom left panel), or Pax7+ cell abundance (bottom right panel) (n=3). **F)** qPCR analysis suggests that *MEG3* overexpression was sufficient to downregulate several mesenchymal marker transcripts in day 7 CTX-injured muscle (n=3).

Table S1: qPCR expression profiling primers.

Gene name	Forward	Reverse
18S	CATTCGAACGTCTGCCCTAT	CCTCCAATGGATCCTCGTTA
Gtl2	GACTTCACGCACAACACGTT	TTACAGTTGGAGGGTCCTGG
Myf5	CCTGTCTGGTCCCGAAAGAAC	GACGTGATCCGATCCACAATG
MyoD	CCACTCCGGGACATAGACTTG	AAAAGCGCAGGTCTGGTGAG
Mef2C	GTGGTTTCCGTAGCAACTCCTAC	GGCAGTGTTGAAGCCAGACAGA
Myog	GAGACATCCCCCTATTTCTACC	GCTCAGTCCGCTCATAGCC
Ckm	GGCTTCACTCTGGACGATGTCA	CCTTGAAGACCGTGTAGGACTC
Acta1	ACCATCGGCAATGAGCGTTTCC	GCTGTTGTAGGTGGTCTCATGG
MEG3	TTGAGTAGAGACCCGCCCTC	CTGTGCTTTGGAACCGCATC
Cdh1	TGCAGGTCTCCTCATGGCTTTG	CTTCAAATCTCACTCTGCCCAGG
Cdh2	ACTTGAGAGCACATGCAGTGG	CATACGTCCCAGGCTTTGATCC
Plakophilin	TGAGTCACTCCAACCGAGGTTC	CTTGAGGGTCCCATTGTAGATCGG
PatJ	AGTGTAGCAGACAGGGATCACAG	CACACCGTTTCTGGCAGAGTT
Fibronectin	AGCAAATCGTGCAGCCTCAATC	CTCAGGCTTGCTCTCGCAGTTA
Twist2	AGCAAGAAATCGAGCGAAGATGG	GATCTTGCTGAGCTTGTCAGAGG
Snai2	AACTACAGCGAACTGGACACAC	GTAATAGGGCTGTATGCTCCCGAG
Mmp9	AGTGAGAGACTCTACACGGAGC	CCTGGTCATAGTTGGCTGTGGT
Rian	TCTGAGGTCCATAGCAGAAGATGCC	CCTTTCCGTGCATGGAGATTTGTATCTTG
Mirg	GGCAAGGTCTAGGATGGACA	CGCCAAGCTTCTGAATACTCC

Table S2: ChIP-qPCR primers for enhancer analysis.

ChIP qPCR target: TSS and distal enhancers in the mouse genome with homology to human loci interacting with *MEG3* and Ezh2 reported by Mondal *et al.* 2015		
Primer name	Forward	Reverse
Jag1 distal enhancer	ACTCAGCAGAAATGCATCACAT	AAGGAAAGACTTTTTGAAGAGGGT
Smad2 distal enhancer	CCCCTCTCAGCCCGATCAT	GAACAGGTACTTGGGCAGCAC
Nfatc1 distal enhancer	CTTGGCATAGCAAAAGCAGATGA	TTACGTGGTGTGCACTTTCGT
Smad6 distal enhancer	CTGCGTGCACGTTAGAAACC	CAAAGTGCCGTTAGCAACCC
PDK3 distal enhancer	TGCTCCCTTCTCTGTCCTGT	AACCTCCTCCAGGCTCAGAT
CASK distal enhancer	GAGAGAGTCCTGCCCTGAAC	GTCTTGGATCAGTTCCACTCCA
Chrdl1 distal enhancer	CTGATTACATATTCATCACTCGGGC	GAGGTAGATGATGAAGGCAGGTT
NFIB distal enhancer	GCTACTGACGAGCTGAACACA	CACTTAGGCAATAGATGGCAGTG
Tgfbr1 distal enhancer	GTGTGCTGACTCCTGCATTTC	ACATTGCCGGTGACCGAAG
Olfm1 distal enhancer	AGGGGGAAGCTAGAGACCTG	GAAAGGAGCCTCAGGCCAAA
Fgfr2 distal enhancer	ACTCTGCAGGAGGAGTCAGT	TCTCTTCCTGGTCTGGCTCA
Dock1 distal enhancer	CCAGATACCCTGCCAACAGAT	TTGACTGCACTTCATGGGAGG
IL6st distal enhancer	CCAAAAGCTTCTCCCTTCTCAG	ACTACATGGGTTTGATCTGATCCT
Fgf18 TSS	TGGAGTCCCACACATCACTC	CTAGGAGCTACTGCTTGAGCC
Clmn TSS	CACGCTTGGTGGATACGGG	AGATCAGCGACATCCGTGTG
Smurf1 TSS	TTACGGCCACGGGCT	TGGTCTCCGGCCCAAC
Tnfrsf1b distal enhancer	GTACTTTTAGGTGCTGGGGGA	TGACCAGCAGGTGGGATTTT
Pbx1 distal enhancer	TGTGTGGTCAAGGGGAATCG	ACTAGCGTTCAAGCTGCCAT
Tgfb2 TSS	TAGCACAACCACCGTTGAGAAA	CCCTTTATGGCTCCTTGGGATT
Akt3 distal enhancer	CACATAAGGCAGACTTGTAGGAGG	CTGTATGGTGAGAAGCAGGGTATG
Id4 distal enhancer	TGCATTATGTATTATCCCAGAAGCC	TGCCTCTGTGATGCTCTGAC
Sox4 distal enhancer	AGGCACAACTTGCACCTAATTT	TTGGGCTTAACTGCTTTTTGGTT
Cadm1 distal enhancer	GGGACGTGCTCATCAAAGGA	CCTTTCACTCGGCTGGACTT
Cbx4 distal enhancer	TGAAGCATGTGACCATTTGTGG	TCCCCACTCTCACTCACAGA
Litaf TSS	GATGGGGTGGGGTCTAGGAG	TCAGGTCGTAGCTTCATCCCT

Table S3: ChIP-qPCR primers for TSS analysis.

ChIP qPCR target: transcription start sites harboring H3K27me3 identified in mouse satellite cells by Liu *et al.* 2013.		
Primer name	Forward	Reverse
Adamts13 TSS	AGCAACCCTCAAGGGTGAAG	CTCTGCGTCTGTTGACTCCA
Aldh1a2 TSS	CACGTCCAATAAGAAGCGCC	ATCTCGCTGGAAGTCATGGG
Arg2 TSS	GCTGTAGTCCTCCGAGAAGGT	CTTCGATGCTTCACTAGGCGA
Cdc3 TSS	TCTGGACCCTTTTTAAGCGTGG	CACGGCTAGCTCTTCGGC
Coro1a TSS	CCCCAGGACCATTGAGGTTC	CTATGAGGATGTGCGCGTCT
Cdh11 TSS	CGGAATTAGGGAGCGCATTCT	TTCACCGATTTCCCCGCAA
E2f8 TSS	AAATCACCGCGATGCCAAAG	GGCTTACTGATTGGCTCGGA
Embigin TSS	AATTGCGCTGGGAGCGT	CCCTGTGTACACTTGCTGGTA
Fbn2 TSS	AGAGCACTGTCGGAGACCAA	CTACACCAGGACACCGCAAG
Fhod3 TSS	GGCGTTTCTGCGCGTTGATT	GACAGGGAATGCGAGAGTCGT
Gch1 TSS	TAGCCTCAGCTACAGAGTACGG	AGAGATTGCTGGAGATCTAACTGAC
Gda TSS	CCTCCTGGATGCCAATAGGATT	AACACATCCAAAACCAACGCA
Icam1 TSS	AGAGACTATAAAAGCGCCGCC	ACGGGTTGAAGCCATTGCAG
IL10RB TSS	AGAAACAGAAGCGCGGATTG	GGCGGCCTCAAGCTAAGT
Kcnf1 TSS	TCCAGAGCTTTAAGGCCAGC	GACAGAAGGAGTGTGCCCAA
Lef1 TSS	CAACCCAAAGAAAGGGTGGTTT	CCATCGGGACAGAGAAGGTAAC
Ltbp2 TSS	GTAAGGGCTGTATGGCGTGA	CCTTCGGTTCCCCTTCAGAC
Ltbp4 TSS	GTCACGTTTCGGGCCAAGAT	GACGTCGCGAGTGCTACTTT
Mcoln2 TSS	CTCCTGGAATATCTCCCGCC	GCGCTGTCACGAAGGACT
Mctp1 TSS	AGTTCAGAGCTGCAAGTGCT	AGACTTGGCTGTCTTCGCAA
Mkx TSS	CCGGAGTCGTCTCTGCTTTA	GGGAACATGGATACCGCGT
Mybl1 TSS	ACACCCACCGAACAGGAAAA	GAAGGATGGCGAAGAGGTCG
Pdgfra TSS	GCTTACTGGGACGAACACCA	GCGGGCGACGAATGAAAATA
Pik3ap1 TSS	AAGTGAGAAGTCCACACGACC	TGGCTGCCTGCTTTCGG
Pkp2 TSS	AGTCCCTCCTGGTCACTCC	GTCCAGGTGACCCAGGATCT
Ppp1r14c TSS	GTCGACATATTTCGTGCGCC	GTCGTCCGAGGTGGAGAATC
Ptk2b TSS	TCCTTAAAGGGTGGGGTGTG	GAATTGCAGGCGGCATCTAT
Rnd1 TSS	ACTAGCACACTAGCGCGG	ATAGCGGAGCCTTACGAGC
Sfrp2 TSS	TCGAGTACCAGAACATGCGG	GAACTTCTTGGTGTCCGGGT
Slc9a2 TSS	ACTGGGAGGCAGATGGTTTG	GGAAAAGCGGGATTCTCCCA
Tead4 TSS	CGATTTCCCGCTCTCATCCAG	GGAGGGGACGGTTTTCGG
Tgfb1 TSS	CCCTCCCTCGGGCTACTAA	ACCCACGATGAAAGCAGGC